8.2

A U.S. THUNDERSTORM CLIMATOLOGY BASED ON 25 YEARS OF NLDN OBSERVATIONS (1993-2017)

Thomas L. Koehler
United States Air Force Academy, USAF Academy, CO

1. INTRODUCTION

The long-term characterization of thunderstorm activity in the U.S. has been the focus of countless studies since the early 1900s, from the 10-year thunderstorm day study by Alexander (1915) to the 10-year lightning strike climatology by Holle et al. (2016). The research summarized here employs 25 years of lightning strike data collected by the National Lightning Detection Network (NLDN) to construct a thunderstorm day climatology over the contiguous U.S. Some of the key elements of this study include:

- A period of 25 years (1993-2017), longer than previous NLDN-based studies
- All spatial processing performed using ESRI ArcGIS functions
- Reported times of the lightning strikes in GMT converted to Apparent Solar Time (AST)
- The production of three daily grids at 926m x 926m (0.5nnmi x 0.5nmi: nmi = nautical mile) resolution in a North American Equidistant Conic projection
    - Cloud-to-Ground (CG) flash frequency (Fr)
    - Thunderstorm day using a 9.25km (5nmi) audibility range (T5)
    - Thunderstorm day using a 18.5km (10nmi) audibility range (T10)
- Resulting grids stored in ESRI grid format for easy display in ArcGIS

Figure 1 illustrates how ArcGIS facilitates the overlay of a variety of information onto the results from this research.

The basic assumption in this study is that any point within a given radius of a CG flash would hear thunder. Two such audibility radii were evaluated: 5nmi and 10nmi. These radii are consistent with the distances used to define a thunderstorm (TS within 5nmi) or thunderstorm in the vicinity (VCTS from 5 - 10nmi) in ASOS surface METAR reports when NLDN data are employed. In this study only one lightning strike within a given date was needed to define a thunderstorm day. Figure 2 displays examples of the flash frequency (Fr)

* *Corresponding author address:* Thomas L. Koehler, Dept. of Economics and Geosciences, 2354 Fairchild Drive, USAF Academy, CO 80840-6238; e-mail Thomas.Koehler@usafa.edu

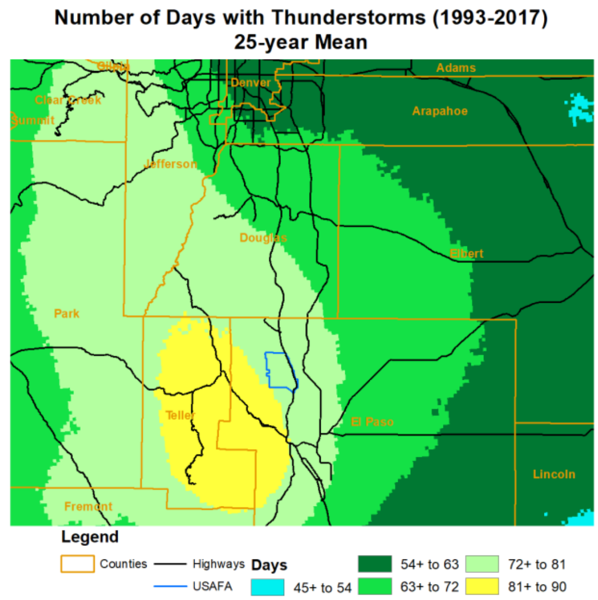

Fig.1. A map of the central Front Range region of Colorado illustrating the 25-year thunderstorm day climatology results with county boundaries, major roads, and the U.S. Air Force Academy boundary superimposed. The yellow region indicating over 81 thunderstorm days per year is centered on Pikes Peak.

and thunderstorm day grids (T5 and T10) produced for one of the 9,095 days included in this study.

2. PROCEDURE

The CG flash data used in this research was downloaded from the NCEI NLDN data archive in daily files (midnight to midnight GMT). The CG flash times were then converted from GMT to AST, adjusting for longitude and the Equation of Time which accounts for variations in eccentricity of the earth's orbit, and the obliquity or tilt of the earth's axis with the ecliptic plane. (See USNO 2015 for the Equation of Time approximation used here.) The time adjustment allows each lightning strike to be placed in a time frame where the sun would be at its highest point in the sky at local noon at any location across the U.S. The lightning flashes were then sorted into daily files, midnight to midnight AST.

Daily processing then ensued. Any CG flashes outside the region of interest (roughly 280 km from the outer edge of the contiguous U.S. – see Fig. 2) were

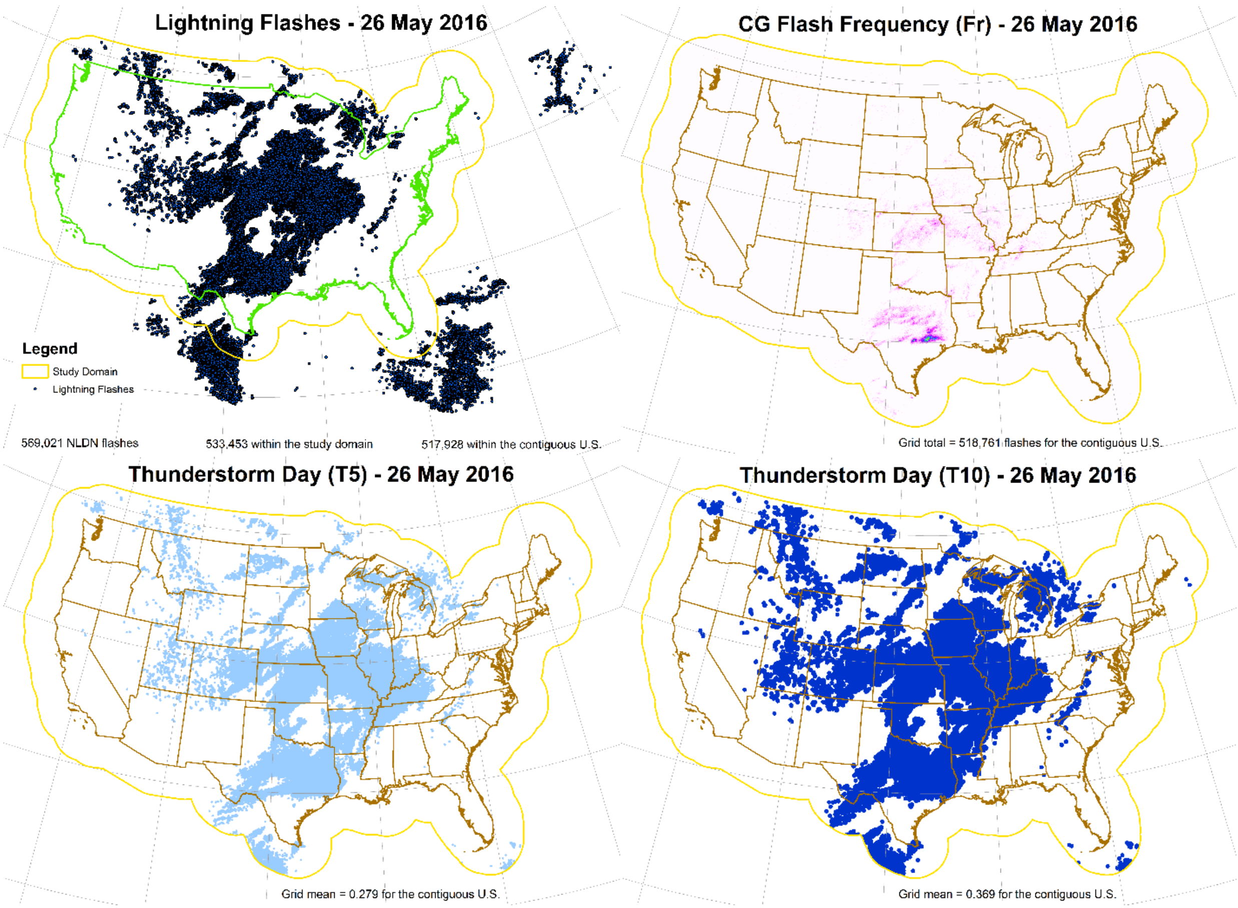

Fig. 2. A one-day sample from the study period (26 May 2016) depicting the original CG strikes (upper left) with the study domain outlined in yellow and the contiguous U.S. map, the CG flash frequency grid (upper right), the thunderstorm day grid using a 5nmi audibility range (lower left - light blue indicating thunder heard), and the thunderstorm day grid using a 10nmi audibility range (lower right - medium blue indicating thunder heard). This date had the greatest number of NLDN lightning flashes in the 25-yr sample with 569,012 flashes.

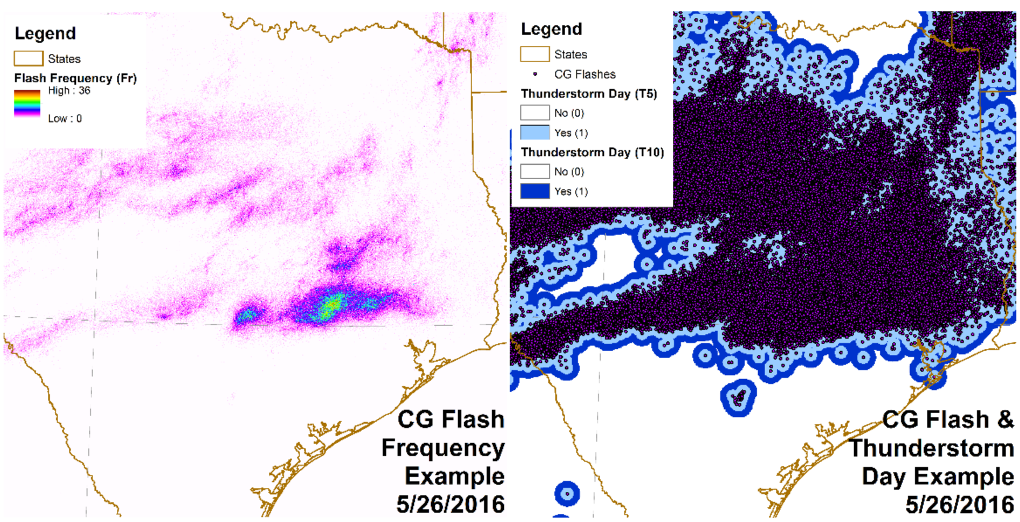

Fig. 3. A close-up of the information from Fig. 2 over Texas. The left panel highlights a region with intense lightning activity in southeast Texas with grid values greater than 30 CG strikes within a grid cell. The right panel shows the thunderstorm day grids with the T5 results displayed on top of the T10 results.

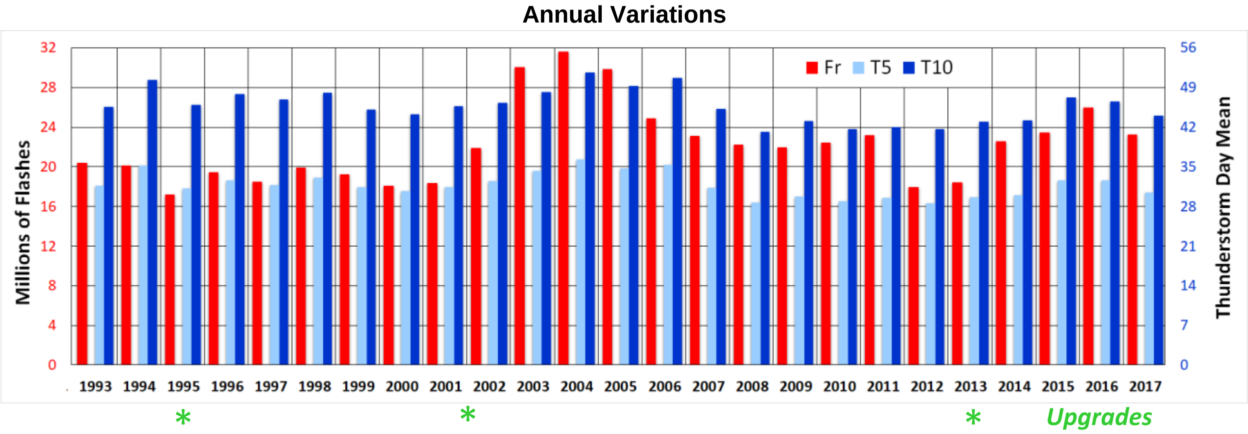

Fig. 4. Annual total number of CG lightning strikes within the contiguous U.S. in millions of flashes (red, left vertical axis), and grid mean number of thunderstorm days (T5 – light blue and T10 – dark blue, right vertical axis) for each year in the 25-year study period. Approximate times of NLDN network upgrades are indicated by green asterisks.

removed. The Point Statistics function of the ArcMap program (ESRI 2018) was then used to define the 926m x 926m grid cell values for the three grids described earlier from the daily lightning flash data points: the number of lightning flashes within each grid cell of the domain (Fr), and whether a given grid cell is within 5nmi (T5) and 10nmi (T10) of a lightning strike. Note that the circular thunderstorm region expected around an isolated lightning flash is resolved well by the 926m x 926m cell size as illustrated in the southwest corner of the regional thunderstorm day map in Figure 3.

The daily Fr, T5, and T10 grid values were then summed for all the days for each of the 300 months in the sample, and the monthly values were summed to create yearly grids. These yearly grids were then clipped to remove grid points outside the contiguous U.S.

3. Results

The following discussions summarize a wide range of results from the study.

3.1 Annual Variations

The annual sums of all the contiguous U.S. grid point values of CG strikes are shown in red in Figure 4. The corresponding grid means of the thunderstorm day grids (T5 and T10) are illustrated in blue in Fig. 4. The total yearly number of CG flashes vary between a minimum of about 17 million flashes in 1995 to a maximum of almost 32 million flashes in 2004. Some of the increase in the annual flash totals in 2003 and 2014 can be attributed to the network upgrades in previous years.

Note also how the grid mean annual thunderstorm days show less proportional variation between the minimum of 29 days in 2012 to a maximum of about 36 days in 2004 for T5, and between a minimum of 41 days in 2008 to a maximum of 52 days in 2004 for T10, than shown in the Fr results. These findings suggest that thunderstorm day variations are less sensitive to changes in lightning detection efficiencies during upgrades than changes in flash frequency, a result consistent with findings from Bourscheidt et al. (2012). They also imply that thunderstorm day statistics provide a more stable measure of thunderstorm activity than lightning frequencies over long periods such as the 25 years used here.

3.2 Monthly Variations

The individual monthly statistics were also combined for each month with the monthly mean calculated by summing the 25 yearly values for a given month and dividing by 25. The resulting monthly mean values are shown in Figure 5. All three variables have peak values in July. The total number of lightning flashes are about equal in the months of June and August, while the grid mean thunderstorm days for T5 and T10 are greater in

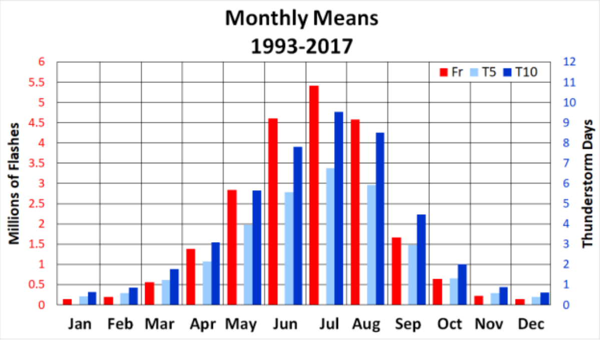

Fig. 5. Monthly mean number of total lightning strikes in the contiguous U.S. in millions of flashes (red, left vertical axis), and grid mean number of thunderstorm days (T5 – light blue and T10 – dark blue, right vertical axis) for each month.

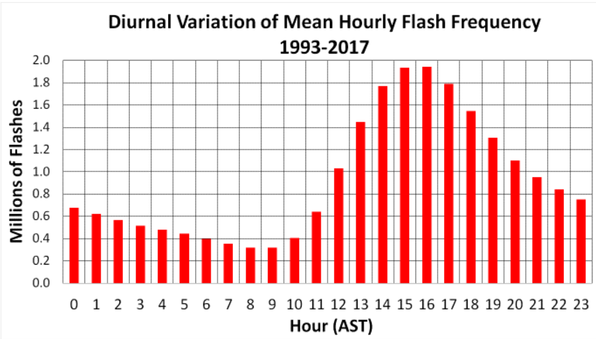

Fig. 6. Hourly mean total lightning flashes over the contiguous U.S. in millions of flashes.

August than in June. The falloff of lightning flashes from August to September also appears to be proportionally larger than the drops in T5 and T10 grid mean thunderstorm days.

3.3 Diurnal Variations in Flash Frequency

The CG flashes over the contiguous U.S. were categorized by hour of the day (AST) during the daily processing, and combined by month and year. The mean annual hourly values are presented in Figure 6. Minimum values of about 0.32 million flashes occur at hours 8 and 9, with a rapid increase to over 1.9 million flashes during hours 15 and 16 AST. These results are quite consistent to the two-hourly results from Holle (2014) for the years 2005-2012, a subset of the 25 years used in this study.

3.4 The Annual Mean CG Flash Density Map

The full-resolution 926m x 926m mean annual CG frequency grid results exhibited a high degree of variability, so the grid values were summed over 4x4 groups of grid cells yielding a coarser grid of flash frequencies at 3704m x 3704m resolution. The values for these cells were then divided by the area of the coarser cell (13.72km^2) to create the flash density map presented in Figure 7.

The overall flash density pattern is very similar to that shown in Figure 1 of Holle, et al. (2016) for the years 2005-2014, with maxima over Florida, the Gulf Coast and eastern Oklahoma. Several locations in California had no CG flashes in the 25-year period, many of them in Monterey County, CA. The maximum value of 17.2 flashes km^{-2} occurred near Tampa, FL in Hillsborough County.

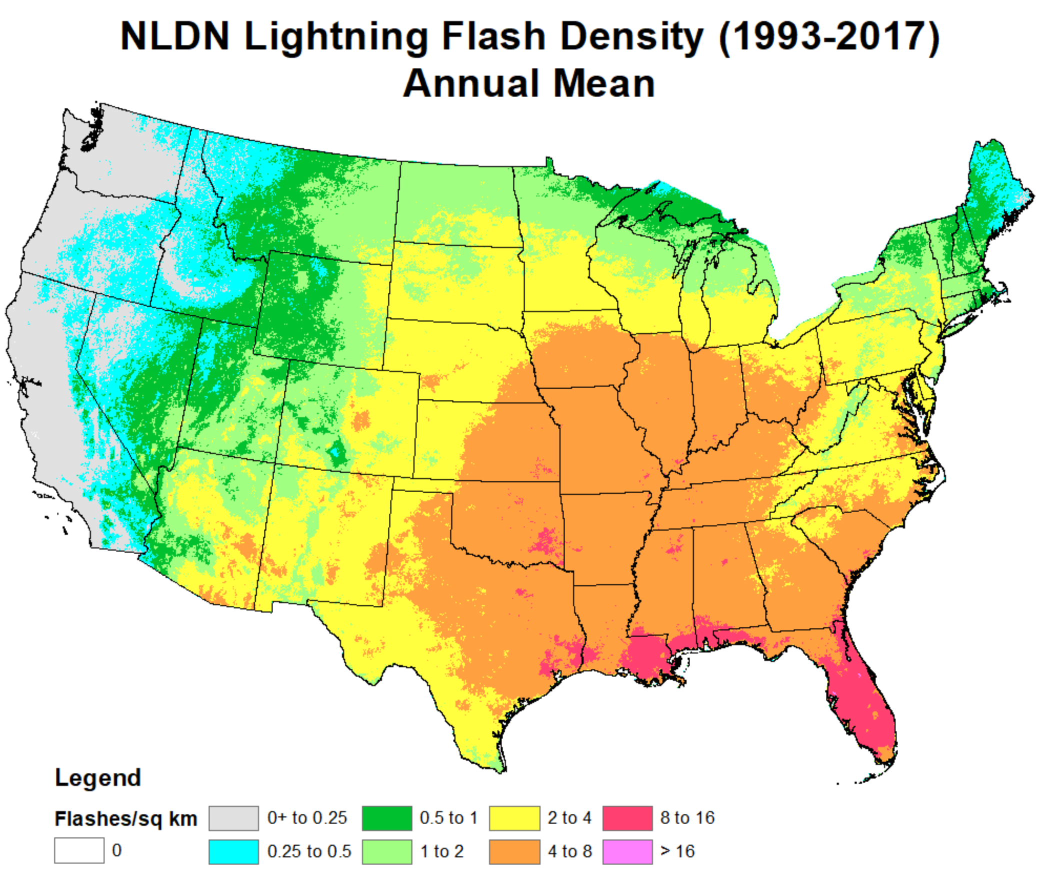

Fig. 7. Annual mean CG flash density map from 25 years of NLDN observations. Note the nonlinear scale.

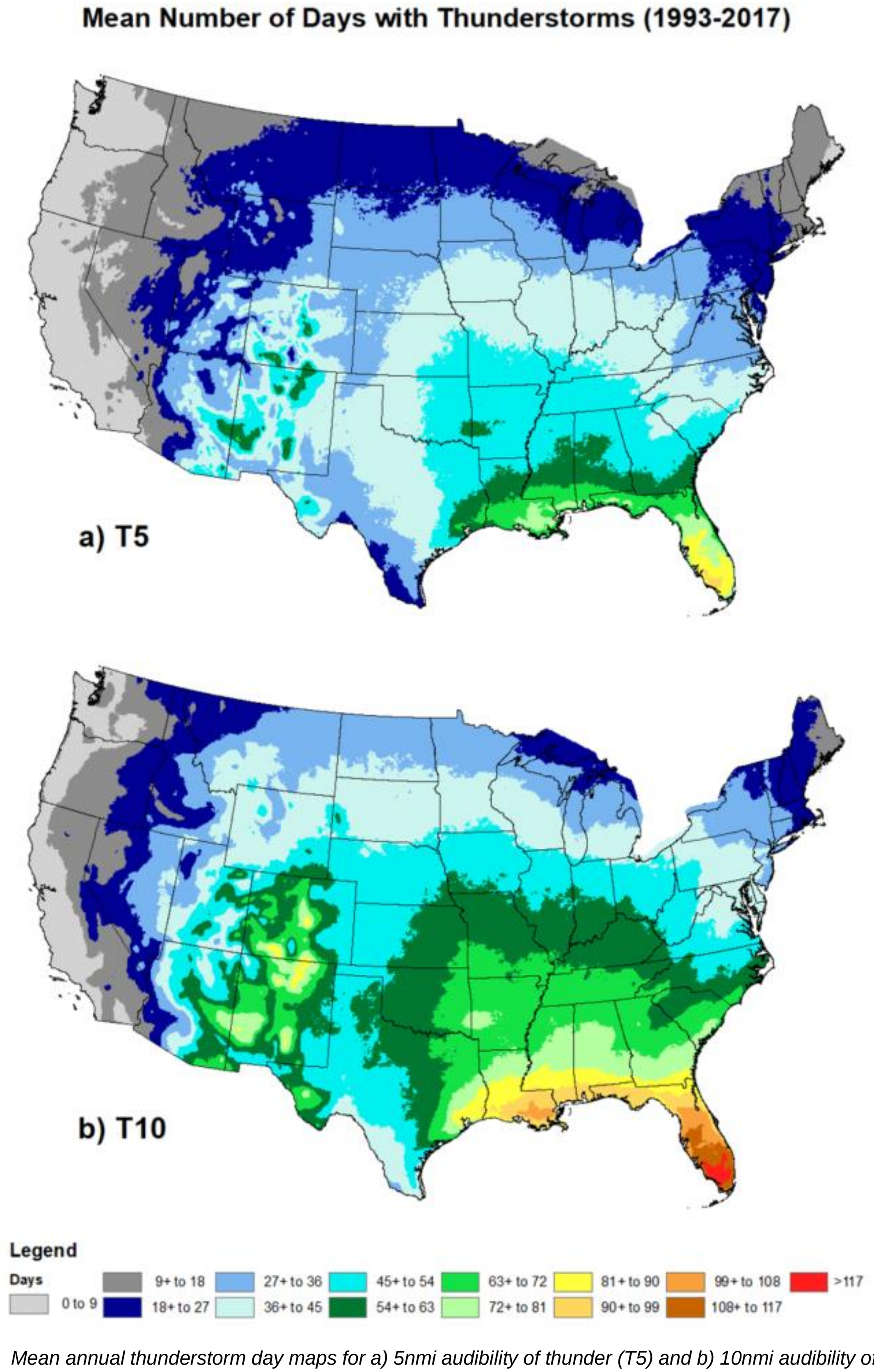

Fig. 8. Mean annual thunderstorm day maps for a) 5nmi audibility of thunder (T5) and b) 10nmi audibility of thunder (T10).

3.5 Annual Mean Thunderstorm Day Maps

Figure 8 on the previous page presents maps of the 5nmi audibility (T5) and 10nmi audibility (T10) thunderstorm day distributions averaged over the 25 years. In both maps the maximum values appear over South Florida with a maximum of 94.5 days for T5 and 123.9 days for T10. Other relative maxima appear over the southern Rocky Mountains reflecting the role played by solar heating of uneven topography in creating the upward vertical motion necessary for the initiation of convection. Generally, thunderstorm day values tend to decrease northward and westward from the Gulf Coast (with the exception of the mountain regions), with values less than 9 days found mostly in the Pacific Coast states.

Comparing the NLDN-derived thunderstorm day distributions in Fig. 8 to similar long-term maps derived from surface observations such as those presented in Changnon (2003) for the 100-year period 1896-1995, and in Court and Griffiths (1986) for the 25-year period 1951-1975 provides interesting insights. The maxima from the surface-based distributions are greater than 90 days, near the maximum for T5, but considerably below the T10 values. An underestimate of thunderstorm activity from surface-based thunderstorm reports when compared to the lightning network estimates was reported in earlier studies by Reap and Orville (1990) and Corborsiero and Lazear (2013).

Another significant difference between surface- and NLDN-based thunderstorm day distributions is over the mountainous western states highlighted in Figure 9. Maxima of over 81 days per year are found over several mountain features in Colorado and New Mexico, including Pikes Peak and the Rampart Range in central Colorado, the San Juan Mountains in southwest Colorado, the Sangre de Cristo Mountains in south central Colorado and northeast New Mexico, the Sacramento Mountains in south central New Mexico, and the Mogollon Mountains of southwest New Mexico. An axis of greater thunderstorm day values extends from this last maximum northwestward into central Arizona along the Mogollon Rim. A local minimum of between 45+ and 54 thunderstorm days is found over the San Luis Valley in south central Colorado. Another discernable maximum is seen in Fig. 8b over the Ouachita Mountains in west central Arkansas and southeast Oklahoma. The correspondence of the thunderstorm day distribution to mountain features is reassuring given the role of topography in thunderstorm initiation. Previous surface observation-based thunderstorm day climatologies were unable to fully illustrate the thunderstorm day maxima over mountains observed in this study due to the relative

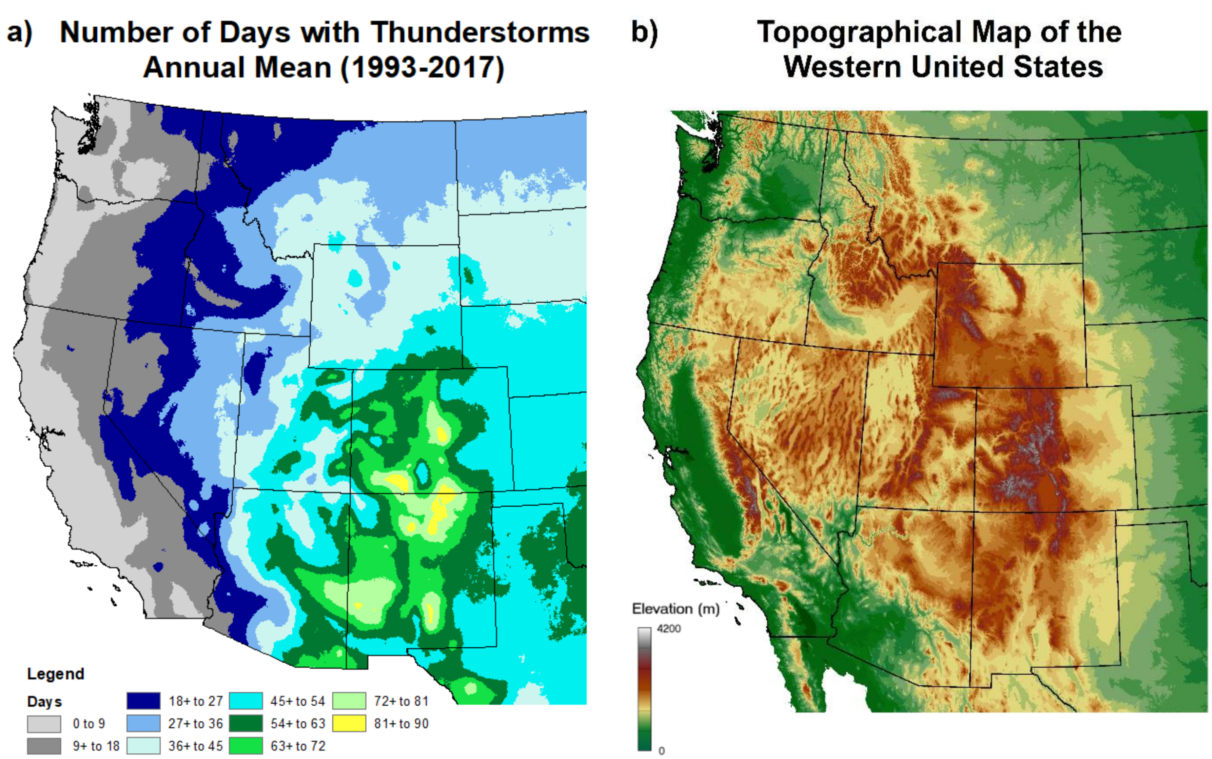

Fig. 9. a) A portion of the T10 map from Fig. 8b for the western United States, and b) a topographical map for the same region.

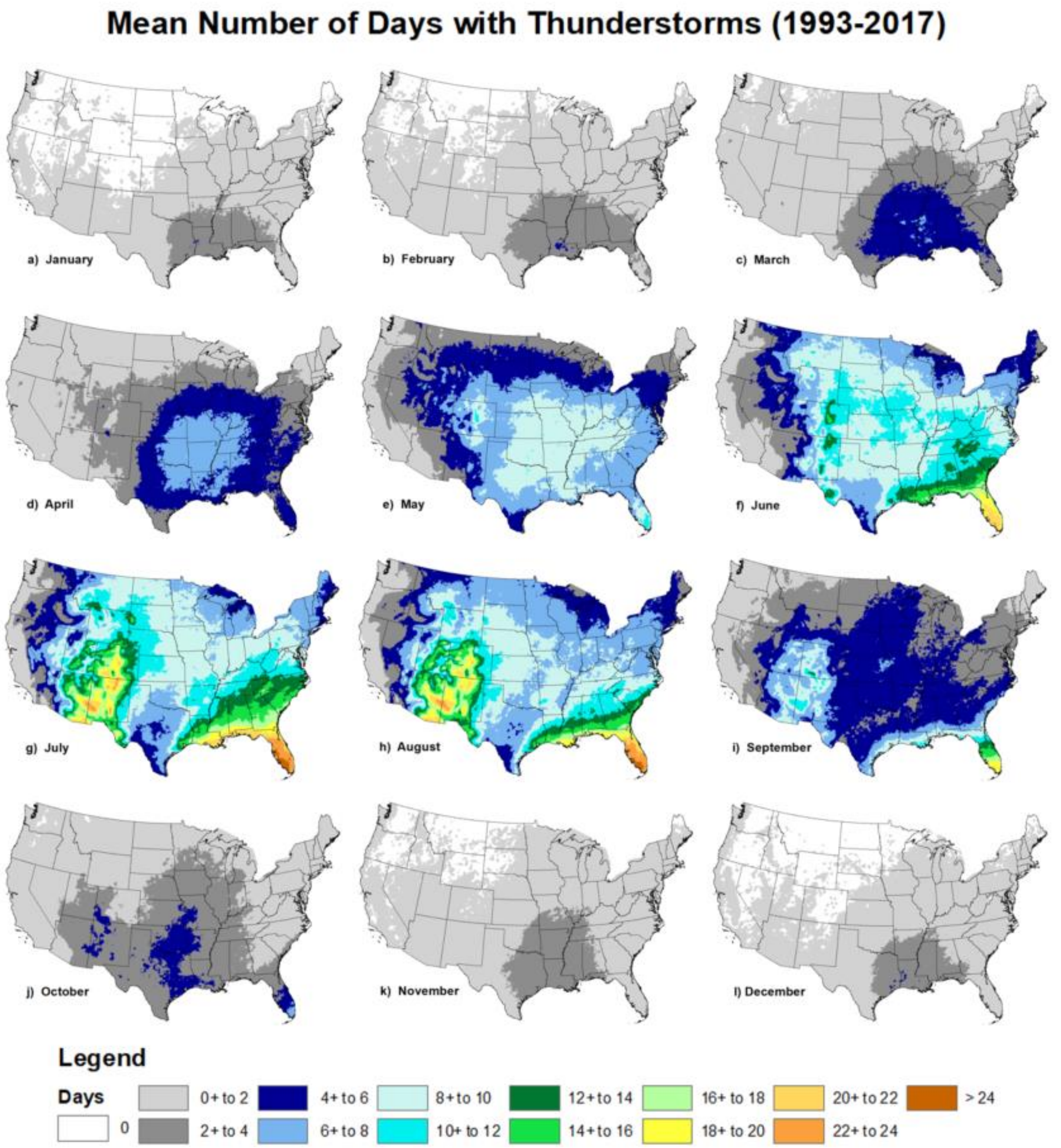

Fig. 10. Monthly mean thunderstorm day maps for 10nmi audibility (T10) for the 25 years 1993-2017. Regions with zero values were without thunderstorm days for the entire 25-year period for that month.

sparseness of surface stations in the western U.S. with 24-hour, long-term data availability.

3.6 Monthly Variations in Thunderstorm Days

Figure 10 shows mean thunderstorm day maps for each of the 12 months. In the four months from November through February, mean thunderstorm day maxima never exceed 5 days per month and appear in the south central U.S. states of Louisiana, Texas, and Arkansas. The March maximum increased to 6.72 thunderstorm days in western Arkansas, and during April the maximum of 8.2 thunderstorm days is located in eastern Oklahoma. By May, a large region covering the southern Great Plains and southern Mississippi Valley has more than 8 thunderstorm days. May maxima of greater than 10 thunderstorm days appear over the Rampart Range and Pikes Peak in central Colorado, in the Red River Valley in Texas and Oklahoma, and over the southern part of the Florida peninsula. Maxima of greater than 20 thunderstorm days remain in Florida from June through September. Values over 18 thunderstorm days extend from Florida through Louisiana along the Gulf Coast, and over the southern Rockies during July and August. Thunderstorm day values decrease significantly in September except in South Florida, and continue to decrease during October.

3.7 Mean Annual Flash Rates

Huffines and Orville (1999), and Makela et al. (2011), took analyses of CG lightning strikes one step further by dividing the flash densities by either thunderstorm days or thunderstorm hours, to obtain a flash rate. Equivalent values were determined for this study. Each flash density grid point value was divided by the corresponding number of thunderstorm days for a 3704m x 3704m grid cell determined by averaging appropriate cells from the 926m x 926m T10 grid shown in Fig. 8b. The result is shown in Figure 11. The maximum annual flash rate of 0.164 flashes km^{-2} TS Day^{-1} is found just east of Orlando, in Orange County, FL. Other flash rate maxima with values exceeding 0.12 are found near Tampa, FL, Biloxi, MS, and in an arc from northeast Texas northward through Oklahoma, eastern Kansas, northern Missouri, then southeastward over Illinois and Indiana. The higher flash rate values can be due to thunderstorms with intense lightning activity, or from long-lived convective systems with long thunderstorm durations within a thunderstorm day.

3.8 Variability of Thunderstorm Day Patterns within the 25-Year Period

The annual, area-averaged T10 thunderstorm day values are repeated in Figure 12, with the series shown in five 5-year periods labeled I through V. Deviations of the 5-year means from the 25-year means (5-year minus

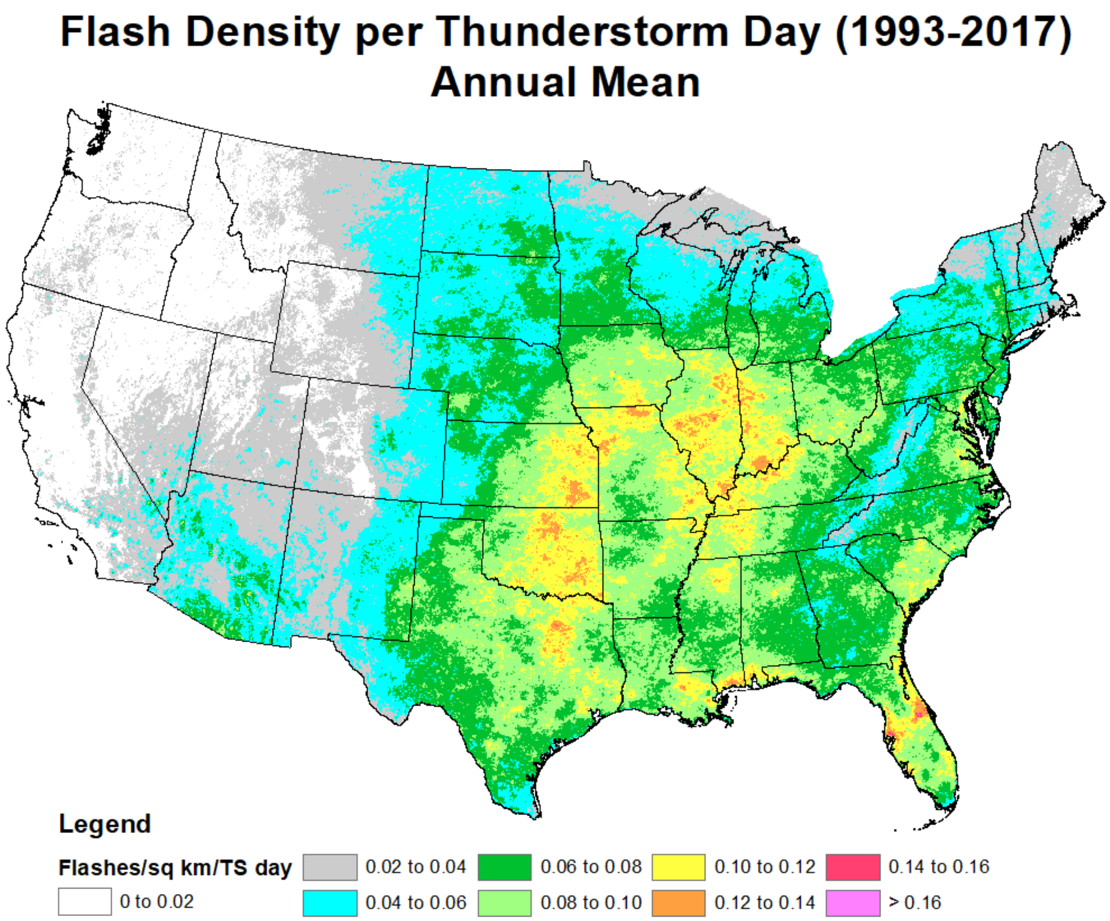

Fig. 11. Map of the mean annual flash density per thunderstorm day for the 25-year period from 1993-2017. Each grid cell has dimensions of 3704m x 3704m (2nmi x 2nmi), and an area of 13.72km^2. Thunderstorm day is abbreviated "TS Day" in the legend.

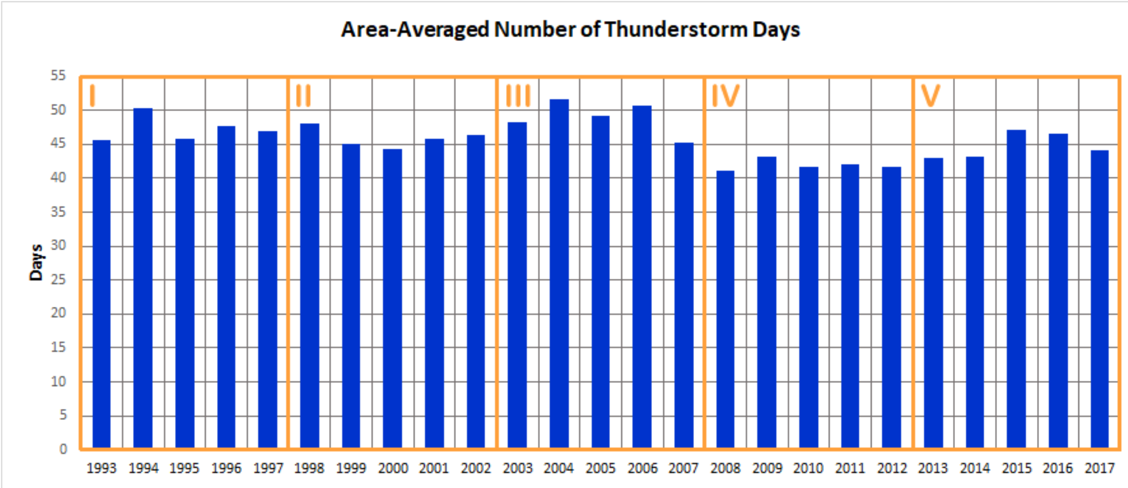

Fig. 12. Grid-averaged annual thunderstorm days for 10nmi audibility (T10) for the contiguous U.S., repeated from Fig. 4. The orange boxes outline the 5-year periods evaluated in this study.

25-year) are shown in Figure 13. The most striking variability is over Texas where large positive deviations of more than 12 days occurred during 2003-2007 (Period III - Fig. 13d), while equally large negative deviations occurred during 2008-2012 (Period IV - Fig. 13e). Period I (Fig. 13b) also shows positive deviations over Colorado and New Mexico extending southeastward into Texas.

3.9 Comparisons with Climate Indices

Several different indices related to interannual climate variability were examined as possible contributors to the variability in thunderstorm days seen in Figs. 12 & 13. Among those examined were the Pacific Decadal Oscillation (PDO) index, the Southern Oscillation Index (SOI), the Atlantic Multi-Decadal Oscillation (AMO) index, and the Multivariate ENSO Index (MEI). Monthly values of these indices were averaged for each year from 1993 to 2017, and the correlation coefficient (r) between each index and the yearly area-averaged T10 thunderstorm days (Fig. 12) was computed. Graphs for the PDO and SOI are presented in Figure 14. The SOI vs. TS Day correlation coefficient was -0.606, the greatest in magnitude of any of the four r values, including that for the other ENSO related index, MEI (r = 0.485, not shown). The r value for PDO vs. TS Day was next largest at 0.477, while the r value for AMO vs. TS Day was -0.037 (not shown).

The SOI (Fig. 14b) is positive during the cold Eastern Pacific phase of ENSO (La Niña) and negative during the warm Eastern Pacific phase of ENSO (El Niño). The negative r for the SOI vs. TS Days implies that a greater number of thunderstorm days would be expected in El Niño years than in La Niña years. Since most thunderstorms occur in the summer, and produce most of the summertime precipitation, surpluses of precipitation might be expected during El Niño periods in regions of positive thunderstorm day deviations, and deficits of precipitation could be expected in regions of negative deviations during La Niña periods. The SOI index for three out of the five years from 1993-1997 (Period I) are negative, implying overall El Niño conditions for that period. The pattern of positive deviations in thunderstorm days apparent in Fig. 13b is in many ways consistent with Figure 15b from Hu and Feng (2012) that shows an axis of positive summertime precipitation anomalies through Colorado and into East Texas and Louisiana during El Niño. All five years of Period IV (2008-2012) have positive SOI values implying La Niña conditions. The pattern of negative deviations in thunderstorm days in Fig. 13e is also consistent with the axis of negative anomalies extending southeastward from Colorado into North Texas during La Niña (Fig. 15c). However the strong positive thunderstorm deviation pattern for Period III (Fig. 13d) has weak SOI index values when small summertime precipitation anomalies might be expected.

4. Conclusions and Future Work

Based on the results shown, the simplification that thunder can be heard within a fixed distance of a CG flash yields reasonable estimates over the relatively long period of 25 years used in this study. The NLDN-derived thunderstorm day patterns over the southern Rocky Mountain region seem particularly more coherent than previous studies based on surface reports of thunderstorms. Overall, the year-to-year variation in grid mean thunderstorm days was less sensitive to lightning detection system upgrades than annual CG flash counts. Thunderstorm activity as determined from NLDN-derived thunderstorm days show some correlation with ENSO, and to a lesser extent, PDO.

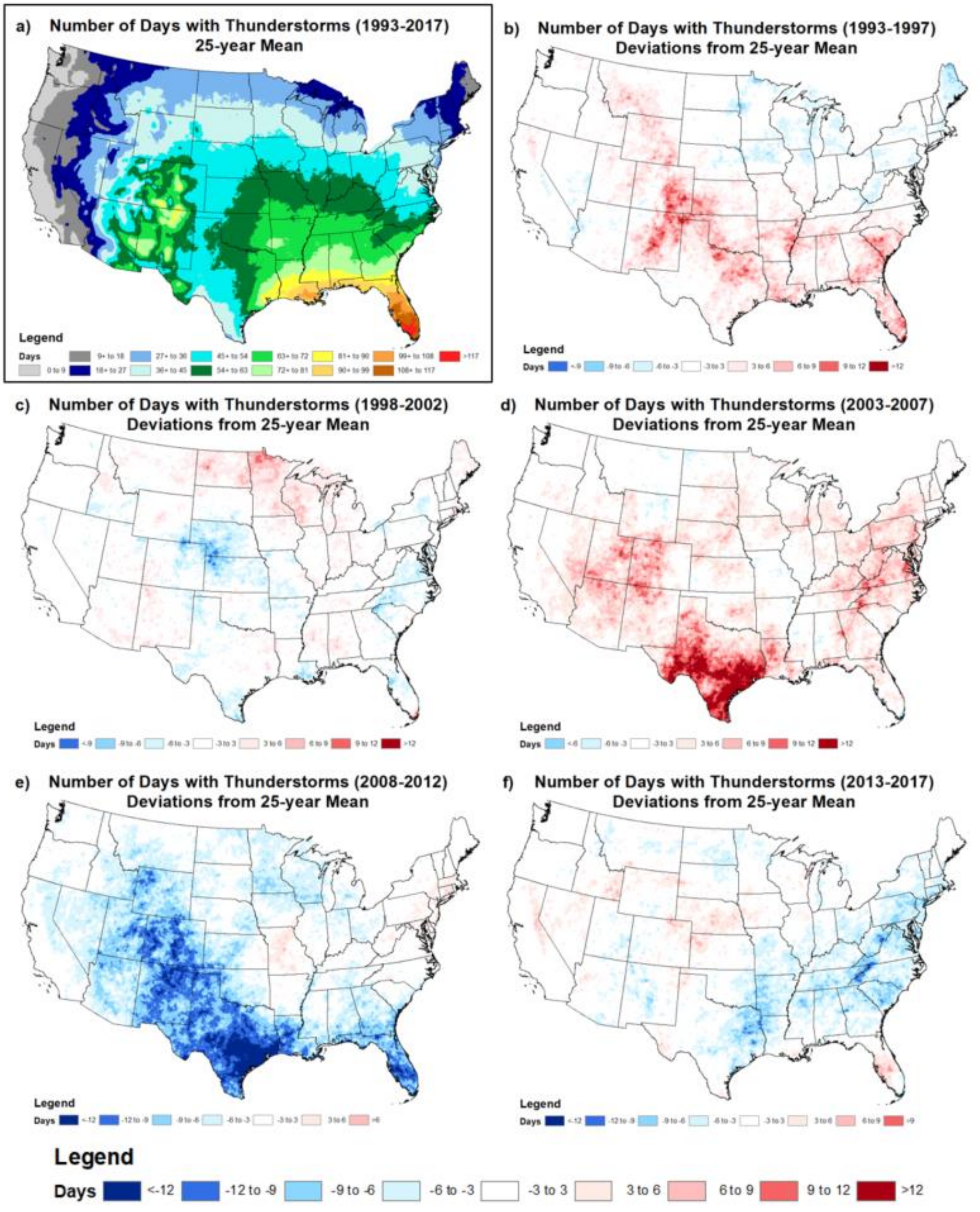

Fig. 13. a) Mean annual thunderstorm day distribution for 10nmi audibility (T10 – same as Fig. 8b), and b) – f), the deviations from this mean for the five, 5-year periods indicated.

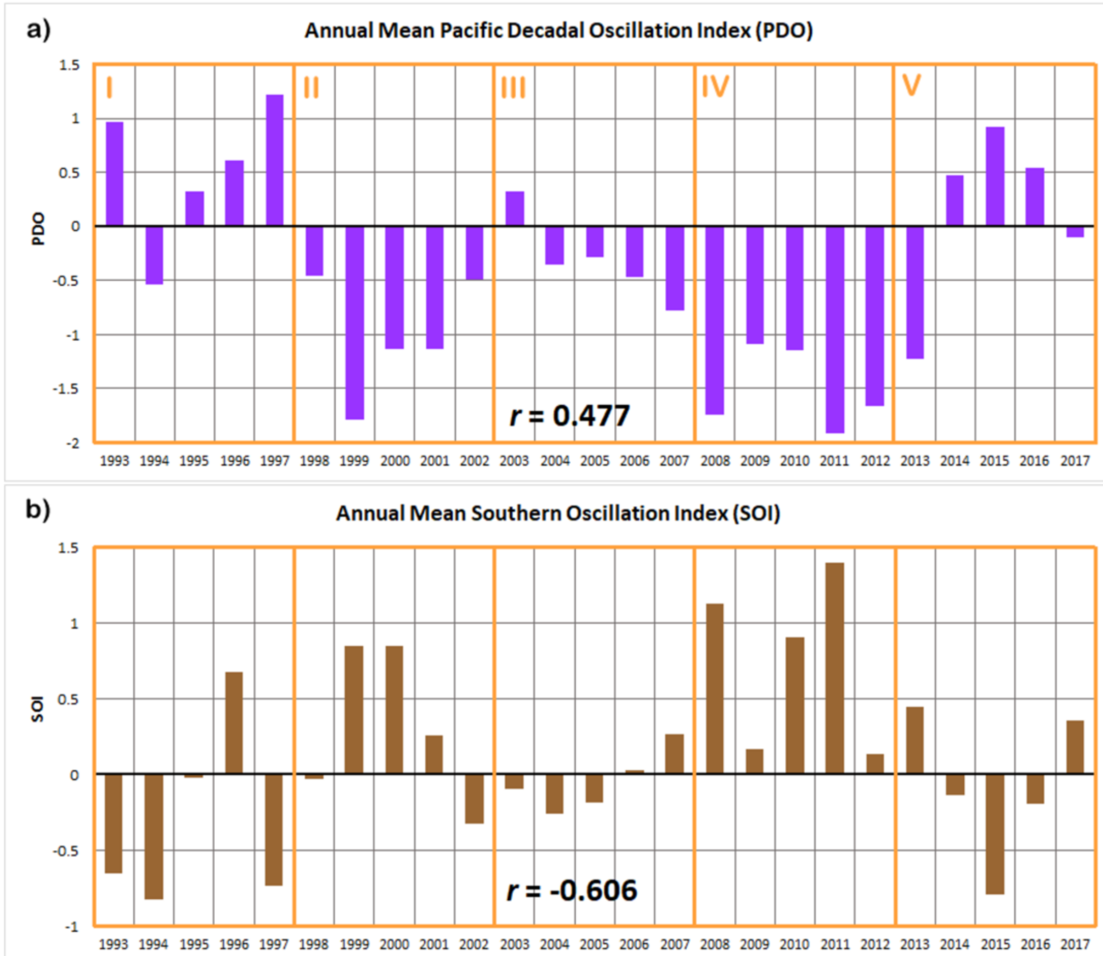

Fig. 14. Plots of the annual mean monthly values of a) the Pacific Decadal oscillation (PDO) and b) the Southern Oscillation Index (SOI) for the 25-year period. Orange boxes delineate the 5-year sub-periods. PDO values tend to be positive (negative) when warmer (colder) waters reside along the Pacific Coast of North America, and SOI values tend to be positive (negative) during La Niña (El Niño) events. The monthly PDO data was obtained from https://www.ncdc.noaa.gov/teleconnections/pdo/, and the monthly SOI data was obtained from https://www.ncdc.noaa.gov/teleconnections/enso/indicators/soi/.

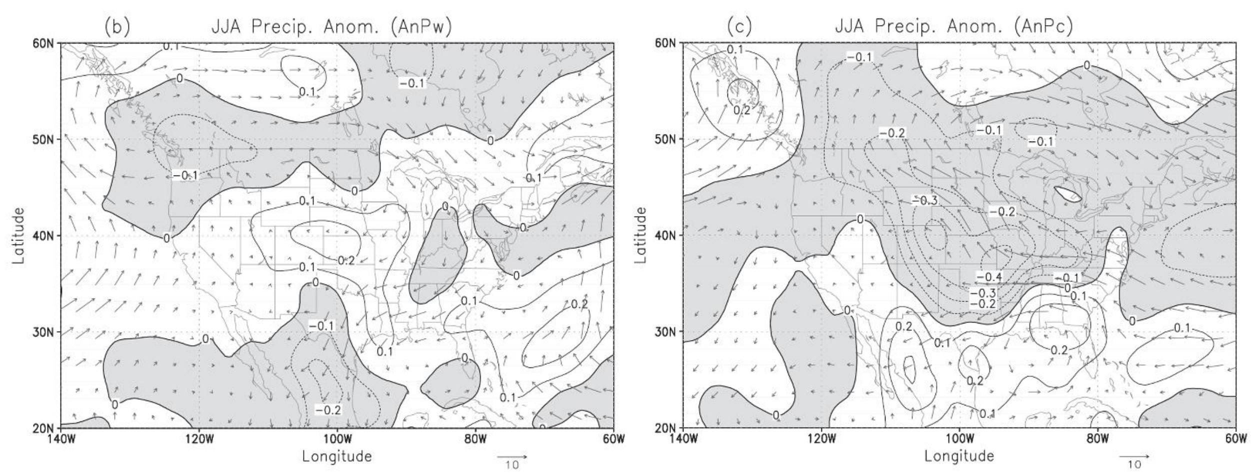

Fig. 15. Panels b) and c) from Figure 8 in Hu and Feng (2012) illustrating simulated summertime precipitation rate anomalies (mm day^{-1}) from ENSO neutral conditions during El Niño (b) and La Niña (c) events.

Future work will examine requiring at least two flashes within the audibility range to indicate a thunderstorm day. This modification will decrease the impact of outlier reports in the NLDN data, and is consistent with the initiation of thunderstorm reports in ASOS processing that uses real-time NLDN information.

ACKNOWLEDGEMENTS

The lightning flash data used in this study were obtained from the NCEI. I thank Mr. Stuart Hinson for facilitating data access. I also thank Col Jennifer Alexander and Lt Col Robert Wacker, faculty colleagues in the Meteorology Program at the U.S. Air Force Academy, for their insightful comments about this research.

REFERENCES

Alexander, W. H., 1915: Distribution of thunderstorms in the United States. *Mon. Wea. Rev.*, **44,** 322-340.

Bourscheidt, V., K. L. Cummins, O. Pinto, Jr., and K.P. Naccarato, 2012: Methods to overcome lightning location system performance limitations on spatial and temporal analysis: Brazilian case. *J. Atmos. Oceanic Technol.,* 29*,* 1304-1311.

Changnon, S. A., 2003: Geographical and temporal variations in thunderstorms in the contiguous United States during the 20th Century. *Physical Geography,* **24**, 2, 138-152.

Corbosiero, K. L., and R. A. Lazear, 2013: Verification of thunderstorm occurrence using the National Lightning Detection Network. Preprints, *Sixth Conf. on the Meteorological Applications of Lightning Data*, Austin, TX, Amer. Meteor. Soc., 8.4. [Available online at https://ams.confex.com/ams/93Annual/webprogram/Paper221132.html.]

Court, A., and J. F. Griffiths, 1986: Thunderstorm climatology. *Thunderstorm Morphology and Dynamics, Vol. 2, 2nd Ed., Thunderstorms: A Social, Scientific, and Technological Documentary*, E. Kessler, Ed., University of Oklahoma Press, Norman and London 9-39.

Environmental Systems Research Institute, cited 2018: "Point Statistics". ArcGIS for Desktop. [Available online at http://desktop.arcgis.com/en/arcmap/10.3/tools/spatial-analyst-toolbox/point-statistics.htm]

Holle, R. L., 2014: Diurnal variations of NLDN-reported cloud-to-ground lightning in the United States. *Mon. Wea. Rev.*, **142**, 1037–1052.

Holle, R. L., K. L. Cummins, and W. A. Brooks, 2016: Seasonal, monthly, and weekly distributions of NLDN and GLD360 cloud-to-ground lightning. *Mon. Wea. Rev.*, **144**, 2855–2870

Hu, Q., and S. Feng, 2012: AMO- and ENSO-driven summertime circulation and precipitation variations in North America. *J. Climate,* 25, 6477-6495.

Huffines, G. R., and R. E. Orville, 1999: Lightning ground flash density and thunderstorm duration in the continental United States: 1989–96. *J. Appl. Meteor.*, **38**, 1013–1019.

Makela, A., P. Rossi, and D. M. Schultz, 2011: The daily cloud-to-ground lightning flash density in the contiguous United States and Finland. *Mon. Wea. Rev.*, **139**, 1323–1337.

Reap, R. M., and R. E. Orville, (1990): The relationships between network lightning locations and surface hourly observations of thunderstorms. *Mon. Wea. Rev.*, **118**, 94-108.

U.S. Naval Observatory, cited 2015: "Approximate Solar Coordinates" [Available online at http://aa.usno.navy.mil/faq/docs/SunApprox.php]